https://doi.org/10.46813/2025-156-061

UDC 621.039.73

CHARACTERIZATION OF MAGNESIUM POTASSIUM PHOSPHATE CEMENT WITH IRON OXIDES ADDITIVES FOR IMMOBILIZATION OF RADIOACTIVE WASTE

S. Sayenko[1], V. Shkuropatenko[1], P. Vecernik[2], V. Kašpar[2], M. Kiselova[2], S. Karsim[1], I. Kolodiy[1], P. Mateychenko[3], K. Lobach[1], A. Zykova[1]

[1]National Science Center "Kharkiv Institute of Physics and Technology", Kharkiv, Ukraine;

[2]ÚJV Rež, a. s., Nuclear Research Institute, Hlavní 130, 250 68 Rež, Czech Republic;

[3]Institute for Single Crystals NASU, Kharkiv, Ukraine

E-mail: shkuropatenko@kipt.kharkov.ua

The effects of adding fine Fe_2O_3 (<5.0 μm) and larger Fe_3O_4 (~44 μm) powders on the hydration, phase composition, microstructure and compressive strength of magnesium potassium phosphate cement (MKPC) was investigated. It was shown that the addition of Fe_2O_3 and its mixture with Fe_3O_4 prolongs the setting time of MKPC paste. The compressive strength of MKPC specimens increased with the increase of Fe_2O_3 content at all curing times. In MKPC with the addition of Fe_2O_3 and Fe_3O_4 mixture, the strength was higher than in the case of the addition of Fe_2O_3 only. XRD analysis revealed that K-struvite $MgKPO_4 \cdot 6H_2O$ was the main phase in the obtained MKPC for all specimens. It was found that the optimized MKPC formulation contained 5 wt.% Fe_2O_3 together with 15 wt.% Fe_3O_4 contributed to the dense microstructure and maximum strength, which are important characteristics to provide long-term waste forms stability.

INTRODUCTION

Composite cementing systems containing high replacement levels of ordinary Portland cement (OPC) with blast furnace slag or fly ash is currently the dominant technical solution for the treatment of low and intermediate level radioactive wastes (L/ILW). These composite systems offer several advantages over OPC alone, including lower heats of hydration, reduced permeability and greater long term durability. However, there are problematic wastes such as spent ion exchangers, borate- and sulfate-containing wastes, organic liquid wastes, and decontamination solutions containing detergent, organic, and/or acidic solutions that cannot be immobilized into existing OPC-based cementitious matrices due to blocking the hydration processes of clinker minerals and cement hardening.

A potential encapsulant for problematic L/ILW waste streams is magnesium potassium phosphate cement (MKPC). Magnesium potassium phosphate cement is a type of chemically bonded ceramic produced through the acid-base reaction between MgO and potassium dihydrogen phosphate, the reaction can be described as Eq. (1):

$$MgO + KH_2PO_4 + H_2O \rightarrow MgKPO_4 \cdot 6H_2O. \quad (1)$$

The chemical reaction resulting in the formation of MKPC (Eq. 1) is based on the dissolution of MgO and KH_2PO_4 reacting in solution to form K-struvite ($MgKPO_4 \cdot 6H_2O$), which is isostructural to struvite ($NH_4MgPO_4 \cdot 6H_2O$) and is naturally cementitious [1]. When compared to the OPC cementing systems, MKPC has advantageous properties including near-neutral pH, low water demand, low drying shrinkage and high early compressive strength [2]. It has a wide range of applications, e.g. solidification/stabilization of heavy metal [3], encapsulation of nuclear wastes [4], repair materials [5], bone materials [6], etc. The widespread use of MKPC at an industrial scale is hampered by certain problems [7]: (1) higher price than OPC; (2) intense temperature evolution during a short hydration period; (3) poor water stability after soaking for a long time.

To improve the properties of MKPC, mineral admixtures in terms of fly ash [8, 1, 9], blast furnace slag [1], silica fume [9], metakaolin [10], etc. are normally added into the MKPC system. Nonetheless, the influence of mineral admixture on the properties of MKPC depends on its type, chemical and physical properties as well as addition dosage. Tan et al. [11] studied the effect of ultrafine fly ash (UFA) and fly ash (FA) on the physical properties, phase assemblage, and microstructure of MKPC. This study revealed that both addition of UFA (D_{50} = 2.69 μm) and FA (D_{50} = 14.0 μm) can prolong the setting time of MKPC paste. Compared with UFA, the addition of FA can increase the setting time of MKPC paste significantly. The addition of a UFA:FA blend can delay the hydration and the setting time of MKPC, enhancing workability. Overall, the optimized formulation was determined to contain 40 wt.% fly ash (10 wt.% UFA and 30 wt.% FA, which achieved the highest compressive strength and fluidity and produced a dense microstructure. The influence of granulated blast-furnace slag fineness on the MKPC characteristics was investigated [12]. It was found that the addition of slag could increase the setting time, which is mainly due to the dilution of cement. Fine slag tends to decrease the fluidity of MKPC mortar. The addition of slag could enhance the early mechanical performance of MKPC mortar due to both the physical filler effect and chemical reaction. The increase in

fineness could further promote the positive contribution of slag to the early strength development of MKPC. The physical contributions of ordinary and ultrafine slag to the early performance of MKPC mortar are 23 and 30%, while the chemical contributions are only 6...10%.

The effects of the addition of Al_2O_3 on the properties of MKPC with respect to changes in temperature, mechanical properties, porosity and microstructure of hydration products is considered in [13]. The experimental results showed that the presence of Al_2O_3 can reduce the intensity of exothermic reactions and prolong the setting time. Also, a significant increase in compressive strength was observed after replacing MgO with Al_2O_3 during all hardening stages. The maximum compressive strength (> 65 MPa), measured after 28 days of curing, was obtained with the addition of 10% Al_2O_3. Furthermore, the addition of Al_2O_3 led to a reduction in porosity, and left a finely porous structure. The substitutions of MgO powder by Fe_2O_3 can reduce the cost of ingredients, reduce the demand for magnesium oxide and improve the properties of magnesium phosphate cement. It was shown that the successive additions of Fe_2O_3 powder led to the improvement of the mechanical properties of magnesium phosphate cement specimens. Specimens with 20% Fe_2O_3 exhibited the highest compressive strength of 25.0; 39.2; 51.9, and 58.7 MPa after curing for 1 h; 1, 7, and 28 days, respectively. Fe_2O_3 powder decreased that fluidity of the fresh paste and prolonged the setting time to a value of 16 min [14]. Red mud is the solid waste in the alumina extraction, mainly consisted of Al_2O_3 and SiO_2, CaO and Fe_2O_3. According to the previous research [15, 16], the optimization results show that the best compressive strength can be obtained when the mass ratio of magnesium to phosphate is 2.7–3.1 and the content of red mud is 10...15%. The 3 h, 1 and 28 days compressive strengths of the optimized specimens can reach 33.4; 53.6, and 75.2 MPa, respectively.

The effect of Fe_2O_3 on the immobilization of liquid high-level waste with MKPC is considered in [17, 18]. The results show that Fe_2O_3 is inert during the hydration reaction. It slows down the hydration reaction and lowers the heat release rate of the MKPC system, leading to a 3...5 °C drop in the mixture temperature during hydration. Early compressive strength of Fe_2O_3 containing specimens decreased slightly while the long-term strength remained unchanged. It has been shown that iron-phosphate forms of waste, if divalent iron oxide (Fe^{2+}) is used, have significant advantages consisting in the ability to immobilize ^{99}Tc for a long time under more reducing conditions [19]. It is also known that the positive effect of the introduced Fe_2O_3 on the attenuation coefficient of MKPC and its ability to shield γ-rays [20].

Iron oxide is one of the most common metal oxides on the planet. Iron oxide has three main forms: FeO, Fe_2O_3 and Fe_3O_4. The most stable and most common of them, and having a lower price, is Fe_2O_3. Hematite Fe_2O_3 given its low cost and abundant reserves in the earth's crust, is considered a promising candidate for partial replacement of MgO in the production of phosphate cements [2]. The choice of magnetite Fe_3O_4 as a replacement addition is due to its prevalence not only in nature, but also in metallurgical waste (mill scale). The addition of iron oxides, including those of varying sizes, can improve the strength and structural characteristics of MKPC specimens.

The present study mainly focuses on the use of fine Fe_2O_3 and larger Fe_3O_4 powders as a material for partial replacement of MgO powder, with an emphasis on optimizing the microstructure and improving the mechanical properties of MKPC. The effects of Fe_2O_3 and Fe_3O_4 replacement additions on the properties of MKPC were determined by measuring the hydration temperature, setting time and compressive strength. X-ray diffraction (XRD), thermogravimetry (DTA-TGA) and scanning electron microscopy (SEM) were used to analyze the phase composition and microstructure. This study can provide useful information for the potential application of MKPC-based materials for the stabilization/solidification of radioactive wastes.

1. MATERIALS AND METHODS

1.1. MATERIALS

The potassium dihydrogen phosphate and magnesia used in the current research were of industrial grade. The purity and providers of the raw materials are listed in Table 1. Magnesium potassium phosphate cement pastes was prepared from a mixture of magnesia (MgO), potassium dihydrogen phosphate (KH_2PO_4), boric acid (H_3BO_3) and iron oxide (Fe_2O_3 or Fe_2O_3/Fe_3O_4 mixture) in various proportions. Hard burnt magnesia powder employed in the present study was calcined at 1100 °C for 2 h in air to reduce reactivity. This powder had a particle size <200 μm. Fe_2O_3 and Fe_3O_4 powder had an average particle size <5.0 and ~44 μm, respectively.

Table 1

Characteristics of raw materials

Component	Purity	Provider
Magnesia (MgO)	Industrial grade, ≥98%	Carl Roth®
Potassium dihydrogen phosphate (KH_2PO_4)	Industrial grade, ≥98%	Carl Roth®
Boric acid (H_3BO_3)	Analytically grade, >99%	PENTA Chemicals Unlimited®
Iron oxide (Fe_2O_3)	Analytically grade, >99%	SIGMA-ALDRICH
Iron oxide (Fe_3O_4)	Industrial grade, 97%	ThermoFisher®

1.2. PASTE PREPARATION AND TEST METHODS

In the present study, the magnesia-to-phosphate (M/P) molar ratio of 2.25 and the water-to-cement (W/C) mass ratio of 0.5 were used to prepare MKPC paste with iron oxides. Nine different dosages of Fe_2O_3 and Fe_2O_3/Fe_3O_4 powder were selected to make MKPC pastes, and details of the mix proportions were listed in Table 2.

Table 2

Mix proportions of MKPC pastes

Batch	Mix propotions, wt.%			Mass ratio		
	MgO	Fe_2O_3	Fe_3O_4	($MgO+Fe_2O_3$(or Fe_2O_3/Fe_3O_4))/KH_2PO_4	H_3BO_3/C	W/C
F0	100	0	0	0.67	0.05	0.5
F5	95	5	0	0.67	0.05	0.5
F10	90	10	0	0.67	0.05	0.5
F15	85	15	0	0.67	0.05	0.5
F20	80	20	0	0.67	0.05	0.5
F15-5	80	15	5	0.67	0.05	0.5
F10-10	80	10	10	0.67	0.05	0.5
F5-15	80	5	15	0.67	0.05	0.5
F0-20	80	0	20	0.67	0.05	0.5

Notations: W/C=Water/ ($MgO+Fe_2O_3$(or Fe_2O_3/Fe_3O_4)+KH_2PO_4).

For the MKPC paste preparation, MgO powder, KH_2PO_4 powder, Fe_2O_3 powder and Fe_2O_3/Fe_3O_4 powder were first weighed and mixed in lab grinding mill machine ALPINE for 10 min according to the mixing proportions (see Table 2). Next, boric acid H_3BO_3 (5 wt.% of the total components $MgO+Fe_2O_3$ or Fe_2O_3/Fe_3O_4 together with KH_2PO_4), as a reaction retarder, was dissolved in distilled water, and a mixture of dry components was added to this solution and mixed with a mechanical stirrer for 3 min. Then, the mixed fresh pastes were cast into the plastic molds. The specimens were demoulded within 24 h followed by air curing at a temperature of 20...25 °C.

The setting time of MKPC pastes was measured using the Vicat needle test. The temperature development of the MKPC pastes was monitored by thermocouples [8]. Before pouring the paste, the thermocouple was installed in the middle of the mold, the volume of which is 27 cm^3. The time of contact of the fresh paste with the thermocouple was taken as the start time of the measurements. Data collection was performed using a registration system consisting of a data logger and a computer, with a registration step of 1 min. The measurement was performed in a room at a constant temperature of 23 °C.

Compressive strength of hardened MKPCs was measured by using the MEGA II-600 DMI-S (FORM+TEST Seidner&Co. GmbH) universal testing machine at a loading rate of 0.25 MPa/s. The specimens were cast in the molds of of 3×3×3 cm cube for measuring compressive strength. Strength of specimens at 1, 7, and 28 days were tested. To determine the behavior of MKPC during heating process, differential thermal (DTA) and thermogravimetric (TG) analyzes were performed on an SDT Q600 V20.9 Build 20 thermal analyzer in the temperature range of 23...600 °C, heating rate of 10 °C/min. The phase composition of the materials was studied by X-ray diffraction analysis (DRON-4-07 Cu K_α with a nickel filter to attenuate the K_β component of characteristic radiation). To identify the phases, the ICDD PDF-2 diffraction database (2004) was used. Crystalline phase quantification was performed using MAUD (Materials Analysis Using Diffraction) software to analyse diffraction data using the combined Rietveld method. Electron microscopic studies of morphology and determination of local composition of the MKPC specimens were carried out by the method of electron probe microanalysis on a JSM-6390LV scanning electron microscope with an AZtechEnergy X-maxn 50 energy-dispersive spectrometer (EDX).

2. RESULTS AND DISCUSSION

2.1. TEMPERATURE EVOLUTION AND SETTING TIME

The effect of replacement of MgO powder by iron oxide powders on the hydration temperature of MKPC pastes is shown in Fig. 1. The values of temperature maximums (T_{Max}), time the maximum temperature reached (t_{Max}) and setting time for MKPC pastes with Fe_2O_3 and Fe_2O_3/Fe_3O_4 additions are summarized in Tables 3 and 4, respectively. As can be seen from Table 3, successive replacement of MgO by Fe_2O_3 led to an increase in the setting time. The setting time of 15 min was obtained for MKPC paste with the addition of 20% Fe_2O_3. At the same time, for MKPC paste without additions, the setting time was 9 minutes. Liu et al. [14] also observed an increase in the setting time of MPC paste from 11 to 16 min with an increase in the Fe_2O_3 addition from 0 to 30%.

Previous studies have shown that MKPC hydration may be more complex than equation (1) [21, 22]. According to current concepts, when MKPC precursors are mixed with water, KH_2PO_4 first dissolves in water, forming an acidic medium. Then MgO dissociates to form Mg^{2+} and release heat. Next, HPO_4^- and Mg^{2+} react to form amorphous and crystalline magnesium phosphates in an exothermic process that overlaps with the ongoing dissolution of MgO. The second exothermic peak is associated with the formation of amorphous hydration products, which begin to reach saturation and crystallize to form $MgKPO_4 \cdot 6H_2O$.

Fig. 1 shows that two temperature maxima T_{Max1} and T_{Max2} are observed during the hydration of MKPC pastes of all the compositions under consideration. The time to reach the first temperature maximum t_{Max1} differs slightly for all MKPC pastes with Fe_2O_3 and is within 7…10 min, as can be seen in Fig. 1,a and Table 3. However, the time to reach the second temperature maximum t_{Max2} differs significantly and depends on the amount of Fe_2O_3 addition.

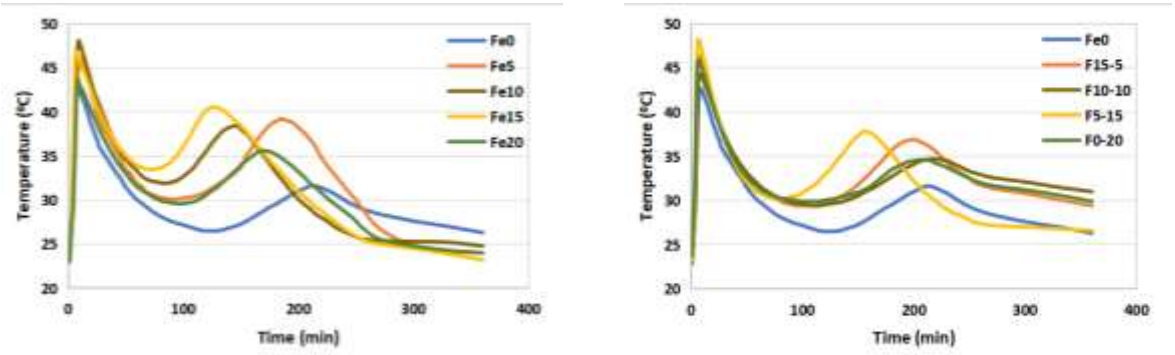

a *b*

Fig. 1. Temperature development of the MKPC pastes with different addition of F_2O_3 (a) and Fe_2O_3/Fe_3O_4 (b) during reaction

With an increase in the Fe_2O_3 addition from 0 to 15%, a decrease in t_{Max2} from 210 to 125 min is observed and an increase to 170 min with 20% Fe_2O_3. The values T_{Max1} of and T_{Max2} of MKPC pastes containing Fe_2O_3 are higher than without Fe_2O_3. The maximum value of T_{Max2} (40.5 °C) with a minimum t_{Max2} (125 min) was recorded for the paste with 15% Fe_2O_3. The decrease in t_{Max2} with an increase in the amount of Fe_2O_3 addition is explained by the fact that it provides a greater number of nucleation sites, which promotes the formation of hydration products, which can accelerate the release of heat. On the other hand, the addition of Fe_2O_3 to the MKPC material as an inert filler replacing MgO reduces the magnesium to phosphate ratio (M/P). As was previously shown [21, 23], a decrease in the M/P ratio led to an increase in t_{Max2}. Probably for this reason, an increase in t_{Max2} is observed with the addition of 20% Fe_2O_3 compared to 10 and 15% Fe_2O_3 (see Table 3).

Table 3

Mix proportion, setting time, maximum temperature (T_{Max}) and the time the maximum temperature reached (t_{max}) of the MKPC pastes with different addition of F_2O_3

Specimens	Fe_2O_3, wt.%	Setting time, min	First maximum temperature		Second maximum temperature	
			T_{Max1}, °C	t_{Max1}, min	T_{Max2}, °C	t_{Max2}, min
Fe0	0	9	42.7	8	31.6	210
Fe5	5	10	45.6	10	39.2	185
Fe10	10	12	48.1	9	38.4	145
Fe15	15	13	46.8	7	40.5	125
Fe20	20	15	43.8	8	35.6	170

In the case of addition Fe_2O_3/Fe_3O_4 mixture, the setting time of MKPC paste increased significantly, as shown in Table 4. With the increase of Fe_3O_4 amount by 5, 10, 15, and 20% in Fe_2O_3/Fe_3O_4 mixture, the setting time of MKPC paste increased to 20, 25, 22, and 35 min, respectively. These results show that the addition of both fine Fe_2O_3 particles and larger Fe_3O_4 particles prolongs the setting time. It is also shown that the addition of large Fe_3O_4 particles has a greater effect on the setting retardation of MKPC pastes than addition of smaller Fe_2O_3 particles. Changing the composition of Fe_2O_3/Fe_3O_4 addition has almost no effect on the time to reach the first maximum t_{Max1}.

Table 4

Mix proportion, setting time, maximum temperature (T_{Max}) and the time the maximum temperature reached (t_{max}) of the MKPC pastes with different addition of F_2O_3/Fe_3O_4

Specimens	$Fe_2O_3+Fe_3O_4$, wt.%	Setting time, min	First maximum temperature		Second maximum temperature	
			T_{Max1}, °C	t_{Max1}, min	T_{Max2}, °C	t_{Max2}, min
Fe0	0	9	42.7	8	31.6	210
Fe15-5	15+5	20	46.4	7	36.9	200
Fe10-10	10+10	25	44.3	8	34.7	215
Fe5-15	5+15	22	48.2	7	37.8	155
Fe0-20	0+20	35	45.9	7	34.6	220

Also, t_{Max2} changes slightly with Fe_2O_3/Fe_3O_4 additions compared to MKPC paste without additions, except for a noticeable decrease in t_{Max2} to 155 min for MKPC paste with the addition of 5%Fe_2O_3+15%Fe_3O_4. In the case of addition the Fe_2O_3/Fe_3O_4 mixture, the presence of smaller Fe_2O_3 particles (< 5.0 μm) led to a decrease in t_{Max2}, while larger Fe_3O_4 particles (~44 μm) cause greater dilution of MKPC precursors and contribute to an increase in t_{Max2}. Therefore, an increase in t_{Max2} from 200 to 215 and 220 min is observed with an increase in Fe_3O_4 from 5 to 10 and 20%, respectively.

2.2. OBTAINING MKPC SPECIMENS AND THEIR COMPRESSIVE STRENGTH

As is known, one of the main factors determining the characteristics of MKPC is the ratio of water to cement (W/C) and MgO to KH_2PO_4 (M/P). Similar to other more traditional cementitious materials the effects of W/C on the properties of MKPC paste are clear, i.e., higher W/C can lead to higher porosity, lower strength, better workability, and longer setting time [24–26].

In turn, the activity of MgO powder has a significant effect on the setting time and hydration temperature of MKPC. Previous studies [27, 28] have shown that the average particle size of MgO increases and the specific surface area decreases with increasing calcination temperature. The smaller is the surface area then the lower is both the reactivity and the slower the reaction. Of course, higher calcination temperatures lead to higher prices for the MgO. In this study, to reduce the activity of MgO, calcination was carried out at a relatively low temperature of 1100 °C. The MgO powder obtained after annealing has a fairly large specific surface area and an increased amount of water is required for its complete wetting and to ensure the workable state of the MKPC paste. Therefore, a high W/C ratio of 0.50 was chosen. In addition, Xu et al. [29] indicated that low W/C ratio slowed down cement hydration at lower M/P beyond 1 day, and prevented the precipitation of intermediate hydrates at higher M/P. At lower M/P expansion and strength loss were observed with time due to the continuing hydration within the already hardened cement.

While the effect of W/C has been clear, experimental results of the effect of M/P in the literature seem to be inconsistent. Chau et al. [30] show that the mechanical properties of the cement pastes are influenced by the crystallinity and growth of magnesium potassium phosphate hexahydrate $MgKPO_4 \cdot 6H_2O$. It was demonstrated that a poor crystal growth and a significant amount of unreacted raw materials would be found in the MKPC pastes with low M/P ratios, while a better crystal growth associated with high early strength can be achieved for the pastes with high M/P ratio. Wang et al. [24] pointed out that with the increase of MgO-to-KH_2PO_4 weight ratio, its compressive strength increased firstly and then decreased. The low compressive strength in lower MgO-to-KH_2PO_4 ratio might be explained by the existence of the weak phase KH_2PO_4. However, the low value of compressive strength with the higher MgO-to-KH_2PO_4 ratio might be caused by lack of the joined phase in the hydrated product.

In practice, higher M/P ratios are more often used in the production of MKPC materials for infrastructure applications [8, 31]. MKPC based composites with low M/P ratios are used as nuclear waste stabilization/solidification binders [1, 4, 32, 33]. This can be explained by the following conclusion. Excessive unreacted magnesia in MKPC materials, especially those with high Mg/PO_4 molar ratios, normally raises the concern over brucite formation and the consequent detrimental volume expansion. It is known that hydration of MgO into $Mg(OH)_2$ is accompanied by a significant volume increase (by 118%), which can induce notable expansion in hardened cement-based materials and raising questions regarding the long-term evolution of such materials, which contain unreacted MgO, in a humid environment [34].

Taking into account the above, MKPC specimens without iron oxide additions were first obtained and tested for compressive strength at a constant W/C ratio of 0.50 and different M/P molar ratios from 1 to 2.7. The results of strength tests of specimens after 1, 7, and 28 days of curing are shown in Fig. 2. As can be seen, the average compressive strength of MKPC specimens increases with an increase in the M/P ratio from 1 to 2.25, and then decreases when the M/P ratio increases to 2.7.

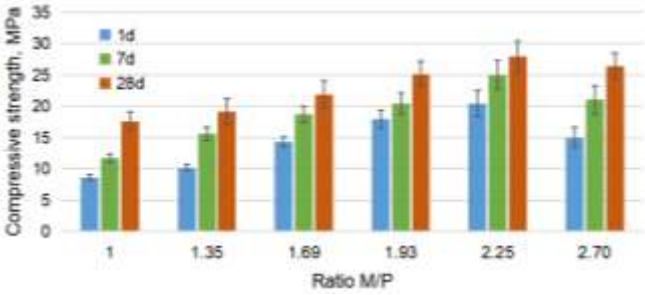

Fig. 2. Compressive strength of MKPC specimens with different M/P ratios

Therefore, when producing MKPC specimens with iron oxide additions, the ratios M/P = 2.25 and W/C = 0.50 were used. The appearance of MKPC specimens with Fe_2O_3 and Fe_2O_3/Fe_3O_4 additions is shown in Fig. 3. None of the specimens showed segregation or cracks, which indicates their good mechanical and physical constitution.

a

b

Fig. 3. Appearance of MKPC specimens (left to right): a – F5, F10, F15, F20; b – F15-5, F10-10, F5-15, F0-20

The improvement of the average compressive strength of MKPC specimens of different compositions after 1, 7, and 28 days of curing is shown in Fig. 4. The average compressive strength value was determined by averaging the strength values of 3 MKPC specimens. The data show that the average strength of MKPC specimens tends to increase with increasing Fe_2O_3 content at all curing times. The highest compressive strength value for F20 with 20% Fe_2O_3 after 1, 7, and 28 days reached 28.0; 29.1, and 31.4 MPa, respectively (see Fig. 4,a).

Previously, an increase in the compressive strength of MKPC specimens with increasing Fe_2O_3 additions was demonstrated by Liu et al. [14]. MKPC specimen with addition of 20% Fe_2O_3 powder showed the highest strength during the whole curing period. Compressive strength after 1, 7, and 28 days of curing was 39.2; 51.9, and 58.7 MPa, respectively. These high strength values were achieved on MKPC specimens obtained at low water-to-cement ratio W/C=0.13. As previously established [7], the compressive strength of MKPC gradually increases with increasing water-to-cement ratio from 0.14 to 0.16. However, with increasing water-to-cement ratio to 0.20, the compressive strength decreases sharply.

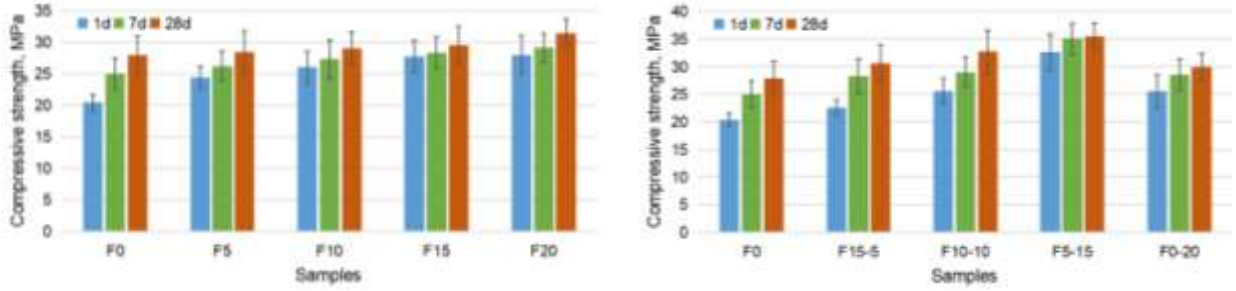

a *b*

Fig. 4. Compressive strength of MKPC specimens with additions: a – Fe_2O_3; b – Fe_2O_3/Fe_3O_4

In MKPC with the addition of a mixture of Fe_2O_3 and Fe_3O_4 (see Fig. 4,b), the compressive strength was higher than with the addition of Fe_2O_3 only (see Fig. 4,a). The maximum average compressive strength after 28 days of curing was 35.5 MPa for F5-15, which is 13.1% higher than that of F20 and 27.2% higher than that of the F0 specimen. As is known in the production of concrete, one of the ways to minimize voids (porosity) is to ensure dense packing by using a set of particles of different sizes and shapes. The pore network of any concrete largely controls the durability of the matrix, and therefore the particles that make up the matrix must be packed as tightly as possible to ensure maximum strength [35]. A similar situation is observed in MKPC specimens. This means that the observed increase in strength is achieved by forming a denser packing of MKPC due to the addition of a mixture of fine Fe_2O_3 and larger Fe_3O_4 powders.

2.3. XRD ANALYSIS

The X-ray diffraction patterns of MKPC specimens F20 and F5-15 after aging for 28 days are shown in Fig. 5,a and b, respectively. K-struvite $MgKPO_4 \cdot 6H_2O$ (PDF #00-035-0812) was the main crystalline product identified in MKPC specimens, in addition to peaks of unreacted periclase MgO (PDF #00-087-0651). In addition to K-struvite and periclase, peaks of hematite Fe_2O_3 (PDF #00-089-8104) were detected in MKPC with added 20% Fe_2O_3. Accordingly, in MKPC with the addition of 5% Fe_2O_3+15% Fe_3O_4 there are peaks of hematite Fe_2O_3 and magnetite Fe_3O_4 (PDF #00-074-0748). Other compounds with clear intensity peaks could not be detected. A small "halo" observed in the angle range of 25...35° in the diffraction patterns indicates the presence of amorphous products in both cases.

Quantitative assessment using the Rietveld method shows that the content of K-struvite and unreacted MgO in MKPC with the addition of 20% Fe_2O_3 (F20) and with the addition of 5% Fe_2O_3 and 15% Fe_3O_4 (F5-15) is approximately equal. Thus, the weight content of K-struvite is 78.2% in F20 and 78.0% in F5-15. The content of MgO: 14.9% in F20 and 14.6% in F5-15. In F20, the total composition of crystalline phases contains 6.9% Fe_2O_3, and in F5-15, 2.6% Fe_2O_3 and 4.8% Fe_3O_4.

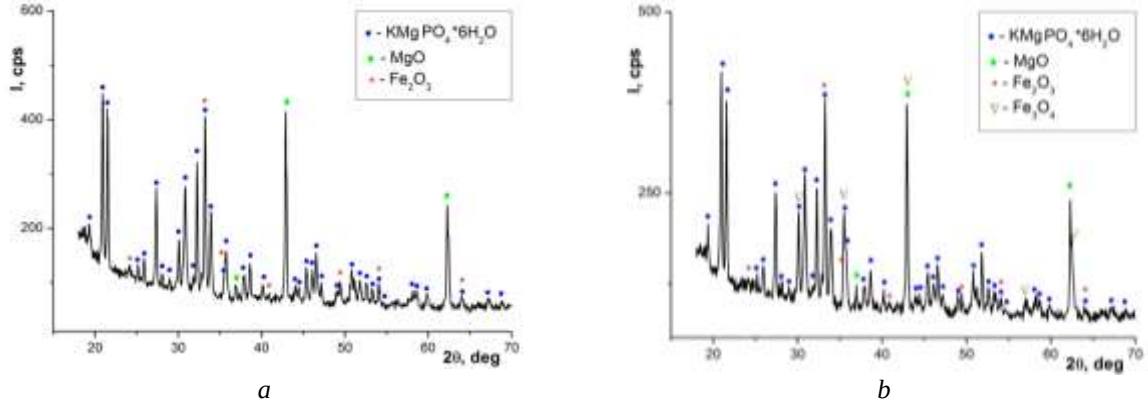

a *b*

Fig. 5. XRD patterns of the MKPC specimens at 28 days of curing: a – F20; b – F5-15

The absence of iron phosphate compounds in the diffraction patterns indicates that что Fe_2O_3 and Fe_3O_4 apparently did not participate in the hydration reaction of MKPC. Therefore, Fe_2O_3 and Fe_3O_4 powders played the role of inert filler in the preparation of MKPC materials. Yang et al. [18] investigated the effects of Fe_2O_3 additions at a dosage of 0, 3, 6, 9. and 12% to replace MgO on MKPC hydration and found iron-containing phases Fe_2O_3 and FeO·OH in the X-ray spectrum of the specimens. However, it was shown that Fe_2O_3 is actually an inert substance for the hydration reaction. As for FeO·OH, it is a product of Fe_2O_3 in an alkaline medium, since MgO was taken in excess with respect to the basic formula of the reaction.

2.4. DTA-TG ANALYSIS

The DTA-TG curves of MKPC F5, F10, F15 and F20 specimens after curing for 28 days are shown in Fig. 6. The DTA curves of all the considered specimens show the presence of the first endothermic peak of low intensity at a temperature near 50 °C and the second endothermic peak of high intensity near 100 °C (see Fig. 6,a). The first peak, according to the data obtained by Xu et al. [22], represents the dehydration of $Mg_2KH(PO_4)_2 \cdot 15H_2O$ (Eq. 2). However, it is not observed by XRD probably due to its low amount (see Fig. 5). The second peak represents the dehydration of K-struvite $MgKPO_4 \cdot 6H_2O$ (Eq. 3) [11].

$$Mg_2KH(PO_4)_2 \cdot 15H_2O \rightarrow Mg_2KH(PO_4)_2 + 15H_2O\uparrow, \quad (2)$$

$$MgKPO_4 \cdot 6H_2O \rightarrow MgKPO_4 + 6H_2O\uparrow. \quad (3)$$

Further on the DTA curve a small exothermic peak near 400 °C is visible. The appearance of this peak without weight loss is associated by the authors [37] with a possible phase transition of β- to γ-$MgKPO_4$ at a temperature of ~420 °C.

As can be seen from the TG curves, the greatest weight loss of specimens F5, F10, F15 and F20 begins at ~70 °C and ends at ~150 °C (see Fig. 6,b), i.e. in the temperature range at which dehydration of K-struvite occurs. This also indicates the presence of an insignificant amount of $Mg_2KH(PO_4)_2 \cdot 15H_2O$ and, as a consequence, its dehydration does not affect the overall weight loss of MKPC. The greatest weight loss is observed for specimen F5, then for specimen F10 and almost identical losses for F15 and F20. This is due to the fact that with an increase in the amount of Fe_2O_3 addition, as an inert filler, from 5 to 10, 15, and 20%, the proportion of K-struvite in the composition of the MKPC material decreases and, accordingly, the loss of mass during dehydration.

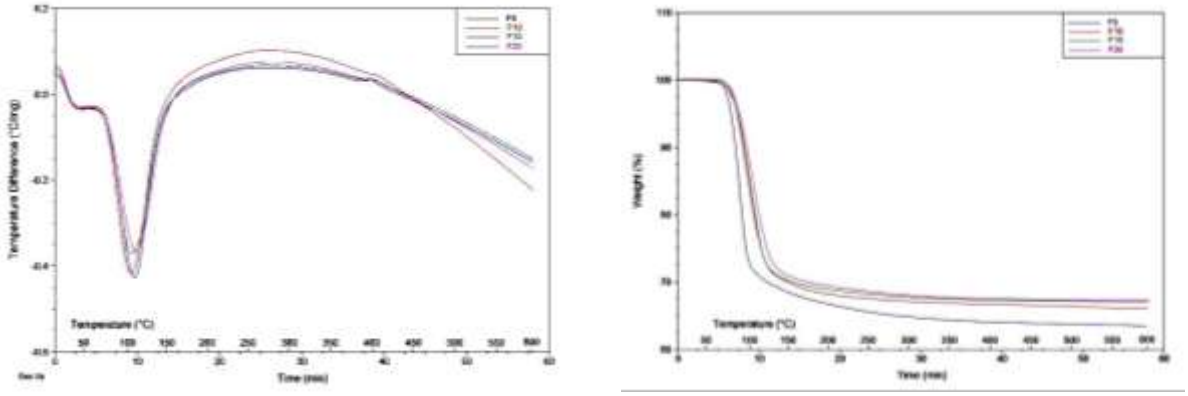

a *b*

Fig. 6. DTA-TG curves of F5, F10, F15 and F20: a – DTA and b – TG

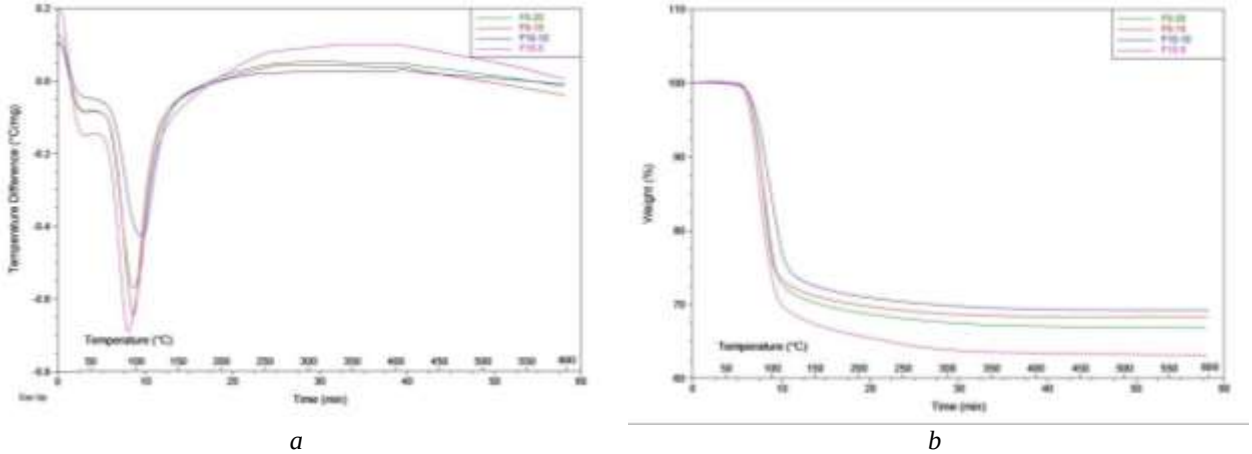

a *b*

Fig. 7. DTA-TG curves of F15-5, F10-10, F5-15 and F0-20: (a) DTA and (b) TG

DTA analysis of MKPC F15-5, F10-10, F5-15, and F0-20 specimens also showed the presence of two endothermic and one exothermic peak (Fig. 7,a). as for F5, F10, F15, and F20 specimens (see Fig. 6,a). The highest mass loss was observed for F15-5 specimen, followed by F0-20, F5-15, and F10-10 (see Fig. 7,b). This suggests that MKPC F15-5 specimen contains more K-struvite, the dehydration of which is mainly responsible for the mass loss, compared to F0-20, F5-15, and F10-10 specimens. As is known, K-struvite is the principal binder that provides mechanical strength of MKPC-based composites

2.5. SEM ANALYSIS

Fig. 8 shows the microstructure of MKPC specimen F5-15, which showed the maximum strength values. It is evident that MKPC has a fairly dense microstructure. The observed microcracks were probably caused by dehydration of the product under vacuum during SEM analysis, as noted in previous studies [1, 38].

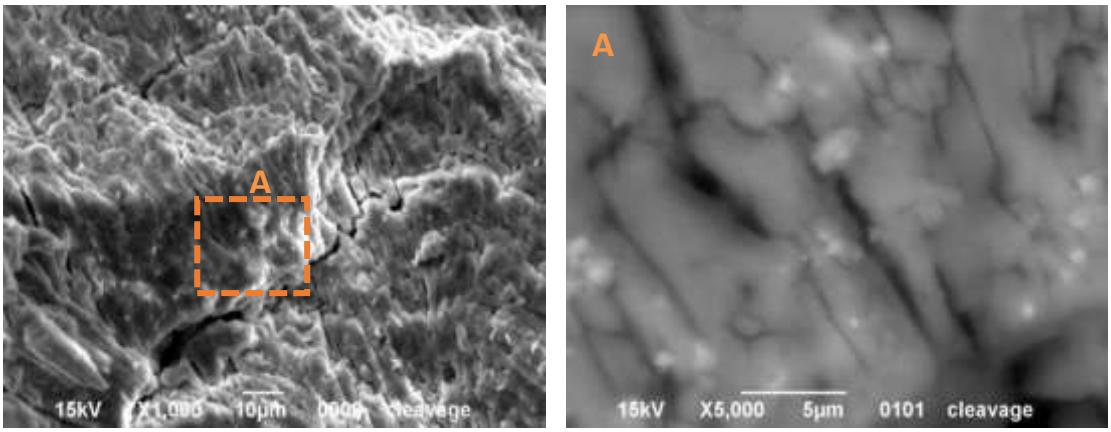

a *b*

Fig. 8. SEM images of MKPC fracture surface: a – specimen F5-15 (secondary electron image); b – with higher magnification (composition images

The secondary electron image of MKPC F5-15 shows the formation of a continuous phase of K-struvite consisting of columnar crystals (see Fig. 8,a). Fig. 8,b shows a backscattered electron image (composition mode) of a fracture surface area of specimen F5-15 with high magnification, and Fig. 9 shows the result of elemental X-ray mapping of this area. Elemental X-ray mapping shows a fairly uniform distribution of the main elements of K-struvite $MgKPO_4 \cdot 6H_2O$: K and P (see Fig. 9,b,c). While areas with increased Mg content are observed (see Fig. 9,a), which is associated with the presence of unreacted MgO particles in the MKPC F5-15 composition, as indicated by the X-ray diffraction data (see Fig. 5,b). The distribution of Fe, as well as Mg, is uneven. The light particles in Fig. 8,b are isolated Fe-containing particles, which is confirmed by the result of X-ray mapping of Fe (see Fig. 9,d).

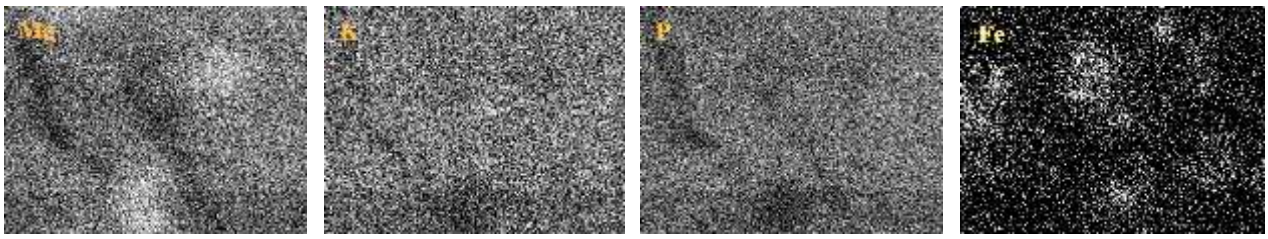

a *b* *c* *d*

Fig. 9. Elemental maps of MKPC F5-15 (area of A)

CONCLUSIONS

This study investigated the effect of partial replacement of MgO by Fe_2O_3 and Fe_2O_3/Fe_3O_4 on the setting time, hydration temperature, compressive strength, microstructure and phase composition of MKPC. Based on the presented experimental results, the following conclusions can be drawn:

1. The addition of fine Fe_2O_3 (<5.0 μm) and larger Fe_3O_4 (~44 μm) powders prolongs the setting time of MKPC paste. The addition of larger Fe_3O_4 powder allows a more significant increase in the setting time compared to the addition of fine Fe_2O_3 powder.

2. The substitutions of MgO powder by Fe_2O_3 powder and Fe_2O_3/Fe_3O_4 powders leads to an increase in the maximum reaction temperatures. The addition of Fe_2O_3 powder reduces the reaction time, while the addition of a mixture of Fe_2O_3/Fe_3O_4 powders does not change it significantly, except for a noticeable decrease in the case of the addition of 5% Fe_2O_3 and 15% Fe_3O_4.

3. Addition of a mixture of 5% Fe_2O_3 and 15% Fe_3O_4 powders increases the compressive strength by 27.2% compared to MKPC without additions. According to the SEM results, a dense microstructure is observed in MKPC with the addition of 5% Fe_2O_3 and 15% Fe_3O_4.

4. According to XRD analysis, K-struvite $MgKPO_4 \cdot 6H_2O$, periclase MgO, hematite Fe_2O_3 and hematite Fe_2O_3 and magnetite Fe_3O_4 were detected in MKPC specimens with the addition of 20% Fe_2O_3 and with the addition of 5% Fe_2O_3 and 15% Fe_3O_4, respectively.

5. As a result of the study, an optimized addition composition was established – 5% Fe_2O_3 and 15% Fe_3O_4. This composition allows to obtain an increased setting time of the paste, a dense microstructure and maximum compressive strength of MKPC, which is one of the key indicators of the quality of protective matrices for radioactive waste.

REFERENCES

1. Laura J. Gardner, Susan A. Bernal, Samuel A. Walling, Claire L. Corkhill, John L. Provis, Neil C. Hyatt. Characterisation of magnesium potassium phosphate cements blended with fly ash and ground granulated blast furnace slag // *Cement and Concrete Research.* 2015, v. 74, p. 78-87; http://dx.doi.org/10.1016/j.cemconres.2015.01.015

2. A.S. Wagh. *Chemically Bonded Phosphate Ceramics, Twenty-First Century Materials with Diverse Applications* / Second Edition, Elsevier, 2016; https://doi.org/10.1016/C2014-0-02562-2

3. Xia Chen, Xian Zhou, Zeyu Fan, Ziling Peng, Qi Lu. Competitive encapsulation of multiple heavy metals by magnesium potassium phosphate cement: Hydration characteristics and leaching toxicity properties // *Waste Management.* 2024, v. 177, p. 115-124; https://doi.org/10.1016/j.wasman.2024.01.046

4. S.Yu. Sayenko, V.A. Shkuropatenko, O.V. Pylypenko, S.O. Karsim, A.V. Zykova, D.V. Kutnii, Arun S. Wagh. Radioactive waste immobilization of Hanford sludge in magnesium potassium phosphate ceramic forms // *Progress in Nuclear Energy.* 2022, v. 152, 104315; https://doi.org/10.1016/j.pnucene.2022.104315

5. Bodong Fang, Zhuojun Hu, Tao Shi, Yanming Liu, Xian Wang, Daping Yang, Kuai Zhu, Xingyu Zhao, Zhifang Zhao. Research progress on the properties and applications of magnesium phosphate cement // *Ceramics International.* 2023, v. 49, p. 4001-4016; https://doi.org/10.1016/j.ceramint.2022.11.078

6. Rita Gelli and Francesca Ridi. An Overview of Magnesium-Phosphate-Based Cements as Bone Repair Materials // *J. Funct. Biomater.* 2023, v. 14, p. 424; https://doi.org/10.3390/jfb14080424

7. Y. Li, B. Chen. Factors that affect the properties of magnesium phosphate cement // *Constr. Build. Mater.* 2013, v. 47, p. 977-983; https://doi.org/10.1016/j.conbuildmat.2013.05.103

8. Biwan Xu, Barbara Lothenbach, Hongyan Ma. Properties of fly ash blended magnesium potassium phosphate mortars: Effect of the ratio between fly ash and magnesia // *Cement and Concrete Composites.* 2018, v. 90, p. 169-177; https://doi.org/10.1016/j.cemconcomp.2018.04.002

9. M. De Campos, C.A. Davy, N. Djelal, M. Rivenet, J. Garcia. Development of a stoichiometric magnesium potassium phosphate cement (MKPC) for the immobilization of powdered minerals // *Cement and Concrete Research.* 2021, v. 142, 106346; https://doi.org/10.1016/j.cemconres.2020.106346

10. Zhaohui Qin, Cong Ma, Zhiqin Zheng, Guangcheng Long, Bing Chen. Effects of metakaolin on properties and microstructure of magnesium phosphate cement // *Construction and Building Materials.* 2020, v. 234, p. 117353; https://doi.org/10.1016/j.conbuildmat.2019.117353

11. Yongshan Tan, Laura J. Gardner, Brant Walkley, Oday H. Hussein, Hao Ding, Shikuan Sun, Hongfa Yu, and Neil C. Hyatt. Optimization of Magnesium Potassium Phosphate Cements Using Ultrafine Fly Ash and Fly Ash // *ACS Sustainable Chem. Eng.* 2023, v. 11, p. 3194-3207; https://doi.org/10.1021/acssuschemeng.2c04987

12. Kuisheng Liu, Shanliang Ma, Zengqi Zhang and Fanghui Han. Hydration and Properties of Magnesium Potassium Phosphate Cement Modified by Granulated Blast-Furnace Slag: Influence of Fineness // *Materials.* 2022, v. 15, p. 918; https://doi.org/10.3390/ma15030918

13. Ning Liu, Bing Chen. Experimental research on magnesium phosphate cements containing alumina // *Construction and Building Materials.* 2016, v. 121, p. 354-360; http://dx.doi.org/10.1016/j.conbuildmat.2016.06.010

14. Yuantao Liu, Bing Chen, Zhaohui Qin, Dong Pen, M. Aminul Haque. Experimental research on properties and microstructures of magnesium-iron phosphate cement // *Construction and Building Materials.* 2020, v. 257, p. 119570; https://doi.org/10.1016/j.conbuildmat.2020.119570

15. Yuantao Liu, Zhaohui Qin, Bing Chen. Experimental research on magnesium phosphate cements modified by red mud // *Construction and Building Materials.* 2020, v. 231, p. 117131; https://doi.org/10.1016/j.conbuildmat.2019.117131

16. Shanliang Ma, Zengqi Zhang, Xiaoming Liu, Yantian Li, Qingsen Zeng, Wei Zhang. Reuse of red mud in magnesium potassium phosphate cement: Reaction mechanism and performance optimization // *Journal of Building Engineering*. 2022, v. 61, p. 105290; https://doi.org/10.1016/j.jobe.2022.105290

17. Lai Zhenyua, Wang Hongtao, Hu Yang, Yan Tao, Lu Zhongyuan, Lv Shuzhen, Zhang Haibin. Rapid solidification of Highly Loaded High- Level Liquid Wastes with magnesium phosphate cement // *Ceramics International*. 2019, v. 45, p. 5050-5057; https://doi.org/10.1016/j.ceramint.2018.11.206

18. Hailin Yang, Mingjiao Fu, Bobo Wu, Ying Zhang, Ruhua Ma, and Jueshi Qian. Effect of Fe_2O_3 on the Immobilization of High-Level Waste with Magnesium Potassium Phosphate Ceramic // *Science and Technology of Nuclear Installations*. 2019, Article ID 4936379, 10 pages; https://doi.org/10.1155/2019/4936379

19. Jongkwon Choi, Wooyong Um, Sungwook Choung. Development of iron phosphate ceramic waste form to immobilize radioactive waste solution // *Journal of Nuclear Materials.* 2014, v. 452, p. 16-23; http://dx.doi.org/10.1016/j.jnucmat.2014.04.033

20. Mona M. Khalil, Mona M. Gouda, Mahmoud I. Abbas, Mohamed Abd-Elzaher & Ahmed M. El-Khatib. Impact of nano Fe_2O_3 on radiation parameters of epoxy reinforced with nano carbon // *Scientific Reports.* 2024, v. 14, p. 21940; https://doi.org/10.1038/s41598-024-73139-8

21. Fei Qiao, C. K. Chau, Zongjin Li. Calorimetric study of magnesium potassium phosphate cement // *Materials and Structures.* 2012, v. 45, p. 447-456; https://doi.org/10.1617/S11527-011-9776-Z

22. Biwan Xu, Barbara Lothenbach, Andreas Leemann, Frank Winnefeld. Reaction mechanism of magnesium potassium phosphate cement with high magnesium-to-phosphate ratio // *Cement and Concrete Research.* 2018, v. 108, p. 140-151; https://doi.org/10.1016/j.cemconres.2018.03.013

23. S. Sayenko, V. Shkuropatenko, Ye. Svitlychnyi, O. Pylypenko, H. Kholomieiev, S. Karsim, A. Zykova. Magnesium potassium phosphate cement for encapsulation of ash from burning radioactively contaminated wood // *Nuclear and Radiation Safety*. 2024, v. 2(102), p. 25-35; https://doi.org/10.32918/nrs.2024.2(102).03

24. Ai-juan Wang, Zhi-long Yuan, Jiao Zhang, Lin-tao Liu, Jun-ming Li, Zheng Liu. Effect of raw material

ratios on the compressive strength of magnesium potassium phosphate chemically bonded ceramics // *Materials Science and Engineering*. 2013, v. 33, Issue 8, p. 5058-5063;
http://dx.doi.org/10.1016/j.msec.2013.08.031

25. Ai-juan Wang, Jiao Zhang, Jun-ming Li, An-bo Ma, Lin-tao Liu. Effect of liquid-to-solid ratios on the properties of magnesium phosphate chemically bonded ceramics // *Materials Science and Engineering*. 2013, v. 33, issue 5, p. 2508-2512;
http://dx.doi.org/10.1016/j.msec.2013.02.014

26. Mathieu Le Rouzic, Thierry Chaussadent, Lavinia Stefan, Mickaël Saillio. On the influence of Mg/P ratio on the properties and durability of magnesium potassium phosphate cement pastes // *Cement and Concrete Research*. 2017, v. 96, p. 27-41;
http://dx.doi.org/10.1016/j.cemconres.2017.02.033

27. Emmanuel Soude´e, Jean Pe´ra. Influence of magnesia surface on the setting time of magnesia-phosphate cement // *Cement and Concrete Research*. 2002, v. 32, p. 153-157;
https://doi.org/10.1016/S0008-8846(01)00647-0

28. Mengliang Liu, Zhenyu Lai, Qiubai Deng, Rui Xiao, Zhi Liu, Xuanzhang Luo, Zhongyuan Lu, Shuzhen Lv. Surface modification of magnesium oxide and its effect on the performance of magnesium phosphate cement // *Construction and Building Materials*. 2022, v. 316, p. 125880;
https://doi.org/10.1016/j.conbuildmat.2021.125880

29. Biwan Xu, Frank Winnefeld, Josef Kaufmann, Barbara Lothenbach. Influence of magnesium-to-phosphate ratio and water-to-cement ratio on hydration and properties of magnesium potassium phosphate cements // *Cement and Concrete Research*. 2019, v. 123, 105781;
https://doi.org/10.1016/j.cemconres.2019.105781

30. C.K. Chau, Fei Qiao, Zongjin Li. Microstructure of magnesium potassium phosphate cement // *Construction and Building Materials*. 2011, v. 25, p. 2911-2917;
https://doi.org/10.1016/j.conbuildmat.2010.12.035

31. Šimon Marušiak, Adéla Kapicová, Adam Pivák, Milena Pavlíková and Zbyšek Pavlík. Magnesium Potassium Phosphate Cement-Based Derivatives for Construction Use: Experimental Assessment // *Materials*. 2022, v. 15(5), p. 1896;
https://doi.org/10.3390/ma15051896

32. Rumu H. Banerjee, Swikisani M.M. Nelwamondo, Naina Raje, Harshala Parab, Nishant Chaudhary, P. Mathi, Jacoba Badenhorst, Amelia Goede, Pranesh Sengupta. Radiation stability testing of hydrated and heat-treated magnesium potassium phosphates for back end nuclear fuel cycle applications // *Ceramics International*. 2024, v. 50, p. 2405-2414;
https://doi.org/10.1016/j.ceramint.2023.11.023

33. Jae-Young Pyo, Wooyong Um, Jong Heo. Magnesium potassium phosphate cements to immobilize radioactive concrete wastes generated by decommissioning of nuclear power plants // *Nuclear Engineering and Technology*. 2021, v. 53, p. 2261-2267;
https://doi.org/10.1016/j.net.2021.01.005

34. Hugo Lahallea, Cédric Patapy, Marwa Glid, Guillaume Renaudin, Martin Cyr. Microstructural evolution/durability of magnesium phosphate cement paste over time in neutral and basic environments // *Cement and Concrete Research*. 2019, v. 122, p. 42-58;
https://doi.org/10.1016/j.cemconres.2019.04.011

35. John L. Provis, Peter Duxson, Jannie S.J. van Deventer. The role of particle technology in developing sustainable construction materials // *Advanced Powder Technology*. 2010, v. 21, p. 2-7;
http://dx.doi.org/10.1016/j.apt.2009.10.006

36. Z. Ding, B. Dong, F. Xing, N. Han, Z. Li. Cementing mechanism of potassium phosphate based magnesium phosphate cement // *Ceramics International*. 2012, v. 38, p. 6281-6288;
https://doi.org/10.1016/j.ceramint.2012.04.083

37. Laura J. Gardner, Samuel A. Walling, Sebastian M. Lawson, Shikuan Sun, Susan A. Bernal, Claire L. Corkhill, John L. Provis, David C. Apperley, Dinu Iuga, John V. Hanna, and Neil C. Hyatt. Characterization of and Structural Insight into Struvite-K, $MgKPO_4 \cdot 6H_2O$, an Analogue of Struvite // *Inorg. Chem.* 2021, v. 60, p. 195-205;
https://dx.doi.org/10.1021/acs.inorgchem.0c02802

38. Liwu Mo, Liming Lv, Min Deng, Jueshi Qian. Influence of Fly Ash and Metakaolin on the Microstructure and Compressive Strength of Magnesium Potassium Phosphate Cement Paste // *Cement and Concrete Research*. 2018, v. 111, p. 116-129; https://doi.org/10.1016/j.cemconres.2018.06.003

Article received 18.03.2025

ХАРАКТЕРИСТИКА МАГНІЙ-КАЛІЙ-ФОСФАТНОГО ЦЕМЕНТУ З ДОБАВКАМИ ОКСИДІВ ЗАЛІЗА ДЛЯ ІМОБІЛІЗАЦІЇ РАДІОАКТИВНИХ ВІДХОДІВ

С. Саєнко, В. Шкуропатенко, P. Vecernik, V. Kašpar, M. Kiselova, С. Карсім, І. Колодій, П. Матейченко, К. Лобач, Г. Зикова

Було досліджено вплив добавки дрібнодисперсного порошку Fe_2O_3 (< 5.0 мкм) та порошку більшого розміру Fe_3O_4 (~ 44 мкм) на гідратацію, фазовий склад, мікроструктуру та міцність на стиск магній-калій-фосфатного цементу (МКФЦ). Показано, що добавка Fe_2O_3 та його суміші з Fe_3O_4 продовжують час схоплювання МКФЦ пасти. Міцність на стиск МКФЦ зразків зростала зі збільшенням вмісту Fe_2O_3 на всіх термінах твердіння. У МКФЦ з добавкою суміші Fe_2O_3 та Fe_3O_4 міцність була вищою, ніж з добавкою тільки Fe_2O_3. За допомогою XRD-аналізу встановлено, що К-струвіт $MgKPO_4 \cdot 6H_2O$ був основною фазою в отриманому МКФЦ для всіх зразків. Було визначено, що оптимізований склад МКФЦ, що містив 5 мас.% Fe_2O_3 разом з 15 мас.% Fe_3O_4, сприяє отриманню щільної мікроструктури та максимальної міцності, які являються важливими характеристиками для забезпечення довгострокової стабільності форм відходів.